

Red Clump Morphology as Evidence Against a New Intervening Stellar Population as the Primary Source of Microlensing Toward the LMC

Jean-Philippe Beaulieu and Penny D. Sackett

Kapteyn Astronomical Institute 9700 AV Groningen, The Netherlands
beaulieu@astro.rug.nl, psackett@astro.rug.nl

ABSTRACT

We examine the morphology of the color-magnitude diagram (CMD) for core helium-burning (red clump) stars to test the recent suggestion by Zaritsky & Lin (1997) that an extension of the red clump in the Large Magellanic Cloud (LMC) toward brighter magnitudes is due to an intervening population of stars that is responsible for a significant fraction of the observed microlensing toward the LMC. Using our own CCD photometry of several fields across the LMC, we confirm the presence of this additional red clump feature, but conclude that it is caused by stellar evolution rather than a foreground population. We do this by demonstrating that the feature (1) is present in all our LMC fields, (2) is in precise agreement with the location of the blue loops in the isochrones of intermediate age red clump stars with the metallicity and age of the LMC, (3) has a relative density consistent with stellar evolution and LMC star formation history, and (4) is present in the Hipparcos CMD for the solar neighborhood where an intervening population cannot be invoked. Assuming there is no systematic shift in the model isochrones, which fit the Hipparcos data in detail, a distance modulus of $\mu_{LMC} = 18.3$ provides the best fit to our dereddened CMD.

Subject headings: Galaxies: Individual (LMC, Sgr) — Galaxies: kinematics and dynamics — Galaxy: halo — Local Group — dark matter — Stars: intermediate age

Accepted for publication in the Astronomical Journal

1. Introduction

The recent discovery of an overdensity of stars in the color-magnitude diagram (CMD) of the Large Magellanic Cloud (LMC) having nearly the same color as the “red clump” of core He-burning stars but extending ~ 0.9 mag brighter has been interpreted as an intervening population of stars at 33 – 35 kpc that may represent a dwarf galaxy or tidal debris sheared from a small Milky Way satellite (Zaritsky & Lin 1997, hereafter ZL). Zaritsky & Lin label this overdensity the VRC (vertical extension of the red clump), and reject other possible explanations to conclude that the VRC represents a massive foreground population with about 5% of angular surface density of the LMC itself. If true, this conclusion would have profound consequences for the interpretation of Galactic microlensing studies (Renault et al. 1997, Alcock et al. 1997a) since such debris could, in principle, be responsible for a sizable fraction of the microlensing signal toward the LMC (Zhao 1996, 1998) that is generally attributed to microlensing by compact objects in the smoothly-distributed halo of the Milky Way itself.

This particular stellar foreground population as an explanation for the LMC microlensing optical depth has been challenged on several grounds. The MACHO team find no evidence for a foreground population at 34 kpc in their extensive photometric database, confirming the LMC membership of their Cepheids (Alcock et al. 1997b, Minniti et al. 1997). They do find an overdensity of stars in a composite MACHO R versus $V - R$ color-magnitude diagram (CMD), but conclude that the *redder* color of this feature is incompatible with the hypothesis of a foreground clump population. (The feature found by MACHO is unlikely to be the VRC, but rather another stage of stellar evolution associated with the asymptotic giant branch.) Gould (1997) argues on the basis of surface photometry of LMC performed by deVaucouleurs (1957) that one of the following is true about any luminous foreground population: (1) it does not extend more than 5° from the LMC center, (2) is smooth on 15° scales, (3) has a stellar mass-to-light ratio 10 times that of known populations, or (4) provides only a small fraction of the microlensing optical depth. Using a semi-analytic method to determine the phase space distribution of tidal debris, Johnston (1998) has analyzed the Zhao (1998) proposition, concluding that an ad hoc tidal streamer to explain the microlensing optical depth toward the LMC would cause unobserved overdensities of 10-100% in star counts elsewhere in the Magellanic Plane or would require disruption precisely aligned with the LMC within the last 10^8 years. Bennett (1997) argues that a recently-determined stellar mass function combined with the assumption that the putative foreground population has a star formation history similar to the LMC results in an implied microlensing optical depth from the VRC that is only a small fraction of that determined by microlensing observations.

We will argue that the VRC feature observed by ZL in color-magnitude diagrams of the LMC originates in the LMC itself. Using BVR CCD photometry of several fields at different locations in the LMC, we confirm the presence of substructure in LMC red clump morphology corresponding to the VRC. In contrast to ZL, however, we argue that the origin is likely to be due to stellar evolution, not an intervening population. We begin by illustrating that the VRC is seen in all our fields. Because the red clump morphology varies slightly in color and magnitude over the face of the LMC, interpretation of composite CMDs is complicated by the superposition of different features. We therefore focus on individual LMC fields, overlaying isochrones and evolutionary tracks of the appropriate metallicity and age in order to demonstrate that the VRC corresponds precisely in magnitude and color to the so called “blue loops” experienced by aging intermediate-mass core He-burning stars. We then show that similar red clump morphology is present in the CMD of Hipparcos, which probes stellar populations on scales of 100 pc from the Sun, where intervening dwarf galaxies or tidal debris cannot be invoked. Finally, we analyze the argument used by ZL to reject stellar evolution as the cause of the VRC, and show that a more realistic model for the star formation history in the LMC is not only consistent with the VRC, but also provides a better fit to the data.

2. New BVR LMC Photometry

In January 1994, Bessel BVR photometry was performed with the Danish 1.5m telescope at ESO La Silla on the EROS#1, EROS#2 and MACHO#1 microlensing candidates and a fourth field was taken far from the bar; we will refer to these fields as F1, F2, F3 and F4 respectively. The detector was a thinned, back-illuminated, AR-coated Tektronix 1024×1024 CCD with a nominal gain of 3.47 e-/ADU, readout noise of 5.25 e-rms, and pixel size of $24\mu m$ corresponding to $0.38''$ on the sky. The detector is linear to better than 1% over the whole dynamic range and is not affected by any large cosmetic defects. Observational and field characteristics are listed in Table I. The CMD of these fields have been used to calibrate data obtained by the EROS microlensing survey, further details can be found in Beaulieu et al. (1995).

We have performed a reanalysis of these BVR data with DOPHOT (Schechter, Mateo & Saha 1993). Typical DOPHOT-reported errors on relative photometry are 0.02 mag at $V = 19$ (typical for the clump stars) for the cosmetically superior (DOPHOT type 1) stars used throughout this analysis. Absolute calibration was performed using Graham (1982) and Vigneau & Azzopardi (1982). Foreground extinction was estimated using H I and IRAS maps (Schwering & Israel 1991); these corrections are listed in Table 1 for each field.

Beginning with this foreground extinction and assuming a metallicity of $Z = 0.008$ for the LMC and a helium abundance of $Y = 0.25$, we then vary the internal extinction to achieve the best fit of the main sequence to the isochrones of Bertelli et al. (1994). In fields F1 and F4, this produces a total extinction equal to that of the foreground (no internal reddening); in fields F2 and F3, the internal extinction results in an additional $E(B - V)_{\text{int}} = 0.04$. We will show that although correcting for extinction is important, the difference between the foreground reddening and the reddening determined from main sequence fitting does not affect our conclusions.

Unless otherwise stated, we assume a distance modulus of $\mu_{LMC} = 18.3$ for the LMC. This choice of distance modulus produces the best fits to the isochrones along the main sequence and in the red clump.

2.1. Features in the LMC color-magnitude diagrams

A calibrated composite $(V - R) - V$ CMD for all four fields is shown in Fig. 1 both with and without extinction corrections for the individual fields. Comparable CMD have been presented and analyzed by Vallenari et al. (1996, and references therein). The red clump is the most notable feature in the LMC other than the main sequence itself and is clearly visible in the composite CMD at about $V_0 \approx 18.7$ and $(V - R)_0 \approx 0.5$ ($(B - V)_0 \approx 0.9$). First identified by Cannon (1970), red clump stars are the counterpart of the older horizontal branch (HB) in globulars, and represent a post helium-flash stage of stellar evolution (for a review, see Chiosi, Bertelli & Bressan 1992). Differential reddening may be responsible for the elongated, tilted red clump in the dustier bar fields F1 and F3, although differences in the age distribution and contamination by the red giant branch bump (see §2.2.4) are also likely to play a role. The morphology of the red clump itself may also be shaped by mass-loss (Renzini & Fusi Pecci 1988, Jimenez, Flynn & Kotoneva 1997). Our analysis is aimed at understanding that portion of red clump morphology relevant to testing the hypothesis that the VRC is due to an intervening stellar population.

2.1.1. The red clump vertical extension (VRC) and supra-clump

A narrow vertical extension of the clump having nearly the same color as the peak red clump density but extending up to ~ 0.8 mag brighter can also be seen. A second source of substructure, or “supra-clump,” is apparent at a position ~ 0.8 mag brighter in V and ~ 0.1 mag redder in $(V - R)$ than the peak of the primary red clump. The positions of these

features are marked in Fig. 1. This substructure can be seen not only in the composite CMD, but also in the calibrated, extinction-corrected $(V - R) - V$ CMDs for each of the individual four LMC fields presented in Fig. 2. Fields F1 and F3 are located close to the LMC bar; fields F2 and F4 further away at about $2 - 3^\circ$ from the center of the LMC. The magnitude and direction of the reddening vector is shown for each field.

Examination of Fig. 2 indicates that although the overall morphology of the CMD is the same in each field, field-to-field variations can be seen in the extent of the red clump and in relative stellar densities along the main sequence and between the main sequence and the red clump. Some of this variation is due to differences in crowding; less severe crowding clearly results in deeper photometry for the F2 field, for example, and thus a larger number of main sequence stars. Since histograms reveal a small relative excess of bright main sequence stars in the outer compared to the inner LMC fields, the star formation history of our fields may also be somewhat different, complicating any analysis that rests on a composite CMD drawn from several regions of the LMC. We therefore choose to analyze the fields independently.

2.1.2. Comparison of with the VRC of Zaritsky and Lin

Using contour plots of our four CMD, we determine the position of the red clump at peak density and the extent of other substructures relative to the clump. The results are summarized in Table 2. The *relative* position of the vertical extension is remarkably constant in each of our fields and is also consistent with that found by ZL: we find that the vertical extension has a $V - R$ color that varies no more than 0.03 mag from that of the primary clump peak and that it extends at least 0.85 mag brighter in V than the red clump peak. The second, redder substructure also maintains a constant relative position to the red clump from field to field. To within 0.02 mag in every field, this supra-clump is 0.85 mag brighter in V and 0.10 mag redder in $V - R$ than the peak density of the red clump.

To test whether the relative stellar density in our CMD within the region of the VRC is consistent with that found by ZL, we return to our composite and individual dereddened $(V - R) - V$ CMD. In color-magnitude space we define the vertical extension ($0.4 \leq (V - R) \leq 0.5$, $17.7 \leq V \leq 18.3$), the supra-clump ($0.5 \leq (V - R) \leq 0.65$, $17.7 \leq V \leq 18.3$) and primary clump ($0.4 \leq (V - R) \leq 0.6$, $18.4 \leq V \leq 19.5$) and count the stars within these regions. These counts are summarized in Table 3, indicating that the VRC represents $\sim 8\%$ and the supra-clump $\sim 14\%$ of the primary clump in the composite CMD. In individual CMDs, the VRC to red clump fraction VRC/RC varies from 6% (in fields F1 and F3) to 15% in field F2. The supra-clump to red clump fraction SC/RC varies

from 12% to 16%. Slightly different choices for the relevant boxes, for example narrowing them to reduce contamination from stars in other stages of stellar evolution, yield very similar fractions. Since our estimate from the composite CMD for the VRC/RC fraction has an uncertainty of $\sim \pm 1\%$ from counting statistics alone, it is consistent with the ZL estimate of $\leq 7\%$ for the relative projected angular surface density of the VRC.

To summarize, the characteristics that we measure for vertical extension to the red clump and the redder supra-clump peak are identical within the uncertainties to those found by ZL and the MACHO team respectively. We therefore identify the vertical feature seen in our data with the VRC discussed by ZL and the redder supra-clump with the overdensity discussed by Alcock et al. In the following section we propose stellar evolutionary origins for each of these features.

2.2. Analysis of the Individual CMDs

The position of red clump stars in a color-magnitude diagram depends on their mass, and thus their age, as they pass through this evolutionary stage. Using the isochrones of Bertelli et al. (1994), we plot in Fig. 3 the mean locus of the core Helium-burning phase for a variety of stellar ages in a $(B - V) - V$ CMD. This time-averaged locus marks where stars in core Helium-burning phase are likely to be found. We have used tracks with metallicity and helium abundance appropriate to the LMC, namely $Z = 0.008$ and $Y = 0.25$. Note that clump stars with ages in the range $\log(\text{Age}) = 8.6 - 9$ (0.4 to 1 Gyr) exhibit color changes smaller than 0.03mag in $(B - V)$ while differing in V magnitude by 0.79 mag. We now compare these theoretical expectations with the VRC in our own LMC data.

2.2.1. Choice of Distance Modulus

We begin by focusing on the field F2, since the low level of crowding in this outer field has resulted in the best photometry of our four fields. The luminosity function for main sequence stars in this field peaks at about $V = 21.5$; in the bar fields this occurs about 0.5 mag sooner. The $(B - V) - V$ CMD for field F2, dereddened by $E(B - V) = 0.12$ is shown in the upper panel of Fig. 4, for two different choices for the LMC distance modulus. Overplotted are theoretical isochrones from Bertelli et al. (1994) computed with new radiative opacities (OPAL) for metallicities appropriate to the LMC ($Z = 0.008$ and $Y = 0.25$) and ages corresponding to 0.25, 0.40, 0.63, 1.0 and 2.5 Gyr ($\log(\text{Age}) = 8.4, 8.6, 8.8, 9.0$ and 9.4). The lower panel enlarges the region of the CMD near the red clump

region, which is now plotted as contours under the mean locus of the core He-burning phase from Fig. 3. Both the fit to the main sequence and the red clump is significantly improved for the smaller distance modulus of $\mu_{LMC} = 18.3$. Since this improvement was apparent in all our fields, we fixed μ_{LMC} at this value.

2.2.2. Importance of Dereddening

Using the same isochrones from Bertelli et al. (1994), ZL concluded that stars of age 2.5 Gyr provided the best fit to the red clump morphology seen in their LMC data. If, following ZL, we do not apply an extinction correction, the 2.5 Gyr isochrone does indeed provide a plausible fit to the red giant branch. With our extinction correction, however, this isochrone falls at the very reddest (or oldest) edge of the red clump in field F2. As Fig. 5 illustrates, this is true for all of our fields. Note that if we had applied only foreground extinction corrections due to the Milky Way itself, the discrepancy with the 2.5 Gyr isochrone would still be present: for two fields the internal extinction (as determined by our main sequence fitting) is negligible, for two others $E(B - V)$ is increased by only 25 - 33%. Furthermore, younger isochrones fit the red clump of each field similarly despite the fact that different external extinction corrections (based on estimates from HI and IRAS data) were made. We take this as an indication that these extinction corrections are reasonable and necessary for the proper interpretation of the stellar evolution.

2.2.3. Identification of the VRC with young He-core burning stars

The He-core burning phase is associated with the horizontal branch in old, metal-poor globulars, but in systems such as the LMC containing stars with a variety of ages and metallicities the horizontal branch becomes blurred into the red clump in CMD. Furthermore, as Fig. 3 makes clear, the horizontal branch actually becomes *vertical* for core He-burning stars of intermediate masses and ages between ~ 0.4 and ~ 1.0 Gyr. Stars of these masses experience the well-known “blue loops” (see e.g., Sweigart 1987, Chiosi et al. 1992) that are caused by the increasing temperature of the outward expanding H-burning shell as the He-burning core gains mass. When the hydrogen in the shell is exhausted and helium begins to burn in the shell, the star moves redward again in the CMD to quickly join the asymptotic giant branch (AGB). While burning helium in their cores and hydrogen in their envelopes, stars spend most of their time near the bluest end of the blue loops. The position of the most blueward extension of the loops for $\sim 2 - 3M_{\odot}$ stars differs substantially in luminosity, but very little in color (Fagotto et al. 1994); in CMD stars of

these masses thus create a vertical extension brightward of the blue end of the red clump.

As can be seen in Fig. 5, all of our fields contain main sequence stars as young as 250 Myr. Since their lifetime on the main sequence is relatively short, intermediate mass stars should also be passing through the core He-burning phase. Indeed, stars with ages between $\sim 0.4 - 0.8$ Gyr lie on a sequence of blue loops whose densely populated blue edge corresponds to the position of the VRC. This is demonstrated clearly in Fig. 6, where the time-weighted centroid of core He-burning stars from Fig. 3 is overplotted on contours of the stellar density for each of our fields. The locus of core He-burning stars agrees with the position of the primary red clump and the vertical extension. The agreement is remarkable, especially considering that we have not adjusted the metallicity of the isochrones to achieve a better fit. We therefore identify the VRC with intermediate mass stars in the LMC currently undergoing core He-burning. In section §2.3 we show that the relative density of stars in the VRC is also consistent with a stellar evolutionary origin.

2.2.4. Identification of the supra-clump with the asymptotic giant branch

The spatial coincidence of the red and asymptotic giant branches with the supra-clump seen both in our data and in the composite CMD of the MACHO database (Alcock et al. 1997b) suggests that this second substructure in the CMD may be associated with giant evolution. Indeed, Zaritsky & Lin (1997) identify the supra-clump with the so-called “red giant branch bump” (RGG, see e.g., Rood 1972, Sweigart, Greggio & Renzini 1989, and Fusi Pecci et al. 1990). During the red giant branch (RGB) phase, color and luminosity evolution pauses as the H-burning shell passes through a discontinuity left by the maximum penetration of the convective envelope. This pause in the ascension results in an overdensity along the RGB. Using an LMC distance modulus of 18.3, the apparent magnitude of RGG stars of $2M_{\odot}$ and LMC metallicities (Sweigart, Greggio & Renzini 1989) agrees with the position and extent of the supra-clump in our data. The same is true using the parameterized models of Fusi Pecci (1990). The position of the RGG is however quite sensitive to stellar age; older stars be fainter when in the RGG phase. The mean age (and metallicity) of the stars will thus determine the position of the RGG for a mixed stellar population.

Recent simulations based on isochrones from OPAL opacities indicate that the RGG may lie at the same magnitude as the red clump itself in the LMC (Gallart & Bertelli 1998) and thus significantly below the position of the observed supra-clump. An alternative explanation for the supra-clump is offered by these simulations: a stalling of the evolution at the base of the asymptotic giant branch (AGB) as the star struggles to reach thermal

equilibrium after the helium exhaustion in the core (Gallart 1998). This early phase of AGB evolution creates an over-density or bump (denoted the AGBB by Gallart) in the CMD since subsequent evolution proceeds much faster along the AGB.

Both secondary features in the CMD are thus explained by stellar evolution: the VRC by young stars of intermediate-mass experiencing core He-burning and the supra-clump by a relatively long-lived phase of He-core exhausted stars at the base of the asymptotic giant branch.

2.3. Relative Stellar Density of the VRC

The position of the vertical extension to the red clump corresponds to the end of the blue loops experienced by intermediate age stars in their He-core burning phase. This argues against the need for an intervening population to explain the VRC, but is the relative stellar density of the VRC consistent with that expected for a stellar population with the star formation history of the LMC?

Comparisons of the stellar density in different parts of the CMD must be done with extreme care due to the selection effects induced by crowding. In addition, comparing regions of the CMD that vary significantly in age increases the chances of error due to uncertainties in the star formation history and the increase of metallicity with decreasing age. For example, comparing the stellar density of the VRC to that of the primary clump not only suffers confusion from the overlapping red giant branch, but also from the tracks of low metallicity old (low mass) clump stars that intersect those of higher metallicity younger (higher mass) clump stars. For these all reasons, we choose to compare the stellar density of stars in the VRC with stars on the main sequence of comparable age and brightness. Our goal is to determine whether simple, reasonable assumptions about the IMF and star formation history of the LMC can reproduce not only the position of the VRC, but its relative stellar density as well.

2.3.1. Choice of IMF and Star Formation History

Detailed models for the stellar density in a particular region of the CMD must combine stellar evolution with assumptions about the star formation history and the initial mass function (IMF) of the population. The LMC is generally believed to be forming stars continuously and to have undergone more star formation in the last few Gyr than previously (see Olszewski, Suntzeff & Mateo 1996 for a review), both on the basis of ground-based

studies (Bertelli et al. 1994, Girardi et al. 1995, and Vallenari et al. 1996) and deeper studies using Hubble Space Telescope (HST) CMD (Gallagher et al. 1996, Holtzman et al. 1997, Elson et al. 1997, and Geha et al. 1997).

As Fig. 7 demonstrates, in each of our four fields, a constant star formation rate with a Salpeter IMF (Salpeter 1955) described by $dN = A M^{-\alpha} dM$ with $\alpha = 2.35$ provides a good approximation to the relative densities of stars on the main sequence down to the completeness limit of $\sim 18.5 - 19$. Field F4 appears to contain a slight excess of very bright main sequence stars (Fig. 5 & 7), which may be indicative of a recent burst of star formation activity. These results are consistent with ground-based and deeper HST studies of the LMC, although most recent work indicates that a slightly steeper IMF provides a better match to the luminosity function at the expense of some relative density ratios (Vallenari et al. 1996, Holtzman et al. 1997, Geha et al. 1997). For the order of magnitude estimates presented here, we will therefore assume that star formation has proceeded at some relatively constant and arbitrary rate between the epochs $8.4 \leq \log(\text{Age}) \leq 9.0$ ($0.25 \leq \text{Age} \leq 1$ Gyr), with $1.85 \leq \alpha \leq 2.85$. Because we will count stars on the main sequence and in the VRC corresponding to the same initial mass, our density analysis is actually independent of the IMF as long as it remains unchanged over this same period. Only when we examine the effects of crowding will slope α of the IMF play a role.

2.3.2. VRC and main sequence counts for intermediate mass stars in the LMC

According to the models of Bertelli et al. (1994), stars with initial masses between 2.6 and $3.0M_{\odot}$ will be ~ 500 Myr old in the red clump where they will have the colors and magnitudes that place them in the center of the VRC. Regardless of its slope, if the IMF is constant over the last Gyr in the LMC, then the ratio of density of these stars in the VRC to their density on the main sequence will depend only on the ratio of lifetimes in these two phases. Here, we define the lifetime in the VRC to be the length of time that these $2.6 - 3.0M_{\odot}$ stars burn helium in their cores and have $0.4 \leq V - R \leq 0.5$. We use the evolutionary models of Fagotto et al. (1994) to estimate the lifetime on the main sequence, which we define as the time during which the fraction of hydrogen in the core is above 0.1%. This definition is operationally convenient since it allows us to count all stars blueward of the subgiant branch. With these definitions, the ratio of VRC to main sequence lifetimes — and thus the ratio of corresponding VRC to main sequence counts — is 23%.

Using these definitions, stars of initial mass in the range $2.6 - 3.0M_{\odot}$ have $-0.15 < V - R < 0.15$ and $19.15 < V < 19.5$ on the main sequence, and $17.8 \leq V \leq 18.5$ in the VRC where their colors are defined as above. Counts in these regions of the CMD

yield VRC to main sequence fractions of 98%, 42%, 61%, and 46% for fields F1 through F4, respectively. Note that the bar fields appear to have the highest VRC fraction. However, since all of our fields are complete at the faintest end of the VRC, but none are complete at $V = 19.5$ on the main sequence, these ratios are overestimated and must be corrected for incompleteness. To estimate the completeness of each field, we compare the actual number of stars found in the main sequence bin to that predicted by a Salpeter IMF normalized to provide good fits to the brighter portion of the main sequence histograms. (For this purpose, main sequence was defined empirically to mean all stars with $0.2 \leq (V - R) \leq (V - 15)^2/80$.) The estimates of the completeness C_{MS} at magnitudes where $2.6 - 3.0M_{\odot}$ main sequence stars would be found are given in Fig. 7 for each field; they range from 42% to 61%. It is difficult to estimate the uncertainty in these completeness estimates, but they are more dominated by counting statistics, which are typically on the order of 15%, than by choice of bins. The resulting VRC to main sequence fractions, corrected for incompleteness, are 59%, 25%, 27% and 19% respectively; all except bar field F1 are in 1.5σ agreement with the prediction of 23% based only on the assumption that the star formation rate and IMF slope have remained constant over the last 1 Gyr in the LMC. The composite completeness-corrected VRC to main sequence ratio is 30%; if the anomalously high field F1 is excluded, this drops to 25%.

The completeness correction assumed a Salpeter slope of $\alpha = 2.35$. A steeper IMF would place more stars on the fainter part of the main sequence and would thus result in larger completeness corrections and smaller VRC ratios. The converse is true for shallow IMF slopes. How well does stellar evolution fare at predicting the 23% VRC to main sequence ratios for $2.6 - 3.0M_{\odot}$ stars if the IMF is modified? Redoing the completeness analysis with a shallow IMF slope of $\alpha = 1.85$ yields a composite VRC to main sequence fraction of 38%. A steeper slope of $\alpha = 2.85$, as preferred by many LMC luminosity function studies (Vallenari et al. 1996, and references therein, Holtzman et al. 1997, and references therein), yields a smaller value of 21%, in excellent agreement with the predicted 23%. Finally, note that stars with masses of $\sim 4 M_{\odot}$, corresponding to ages of 200 Myr in the core He-burning phase evolve so quickly that they would not be expected to be detected in the clump region of the CMD. This may explain the upper magnitude cutoff of the VRC.

In conclusion, stellar evolution combined with a Salpeter IMF and constant star formation over the last 1 Gyr can account for $\sim 75\%$ of the observed stellar density in the VRC. For the somewhat steeper slopes preferred by most recent LMC studies, the fraction rises to 100%. Given the simplicity of the assumptions, counting procedure and incompleteness corrections, this agreement is remarkable and leaves little room for an intervening population of non-LMC stars in this region of the LMC color-magnitude diagram.

3. The Red Clump Vertical Extension in the Hipparcos CMD

The parallaxes obtained by the Hipparcos mission have allowed the determination of distances to stars brighter $M_V = 8$ with accuracies on the order of 10% (Perryman et al. 1997). This has resulted in a more accurately-determined color-absolute magnitude diagram for stars within ~ 100 pc than has heretofore been possible, resulting in the first clear detection of “clump giants” in the solar neighborhood (Perryman et al. 1995). Paczyński & Stanek (1998) conclude from their analysis that the Hipparcos red clump has a mean distance of 105 pc and a geometrical mean distance of 98 pc, making it unlikely that extinction significantly affects the magnitude or color of the clump.

In Fig. 8, we show the color-absolute magnitude diagram for 16229 stars from the Hipparcos catalog with relative distances determined to within 10% and colors determined to within 2.5% (Perryman 1995, and references therein). The red clump is clearly visible as a highly concentrated collection of stars with a density peaking near $V = 0.8$ and $B - V = 1.0$. The fainter, redward tail of the clump seen most clearly in the contours may be due to the evolving core He-burning stars overlapping the giant branch (i.e., pre-helium flash giants).

Also visible in the Hipparcos CMD is a vertical extension of the red clump toward brighter magnitudes; its color is indistinguishable from that of the peak of the red clump. Centered near $V = 0$, this feature is clearly discernible by eye at $-0.5 < V < 0.5$ and $0.9 < B - V < 1.1$. Its presence and location is robust to a variety of different choices for the smoothing and contouring of the CMD. A second overdensity at similar magnitudes ($0.6 < V < -0.6$) but redder colors ($1.2 < B - V < 1.4$) is also apparent, and may correspond to the position of the AGBB.

The isochrones overplotted in the upper panel of Fig. 8 assume a solar metallicity of $Z = 0.02$ for stars of ages 0.4, 1.0, 2.5, 6.3 and 10.0 Gyr. It thus appears that the solar neighborhood has undergone some star formation in the last 400 Myr, but that the bulk of the stars in the red clump in the solar neighborhood are older than those of the LMC. The horizontal extent of the Hipparcos red clump is due to older stars that begin burning helium in their cores at fainter, redder positions in the CMD and experience less severe blue loops. In the lower panel of Fig. 8, the area around the clump is enlarged and the stellar density plotted as contours. The VRC in the solar neighborhood can be seen clearly. Both the isochrones overplotted in the upper panel of Fig. 8 and the theoretical locus of core He-burning stars (of appropriate metallicity) overplotted in the lower panel make it clear that the VRC seen in the Hipparcos data is due to younger clump stars with ages between 300 Myr and 1 Gyr.

4. The CMD Observations used by Zaritsky and Lin

Both our CMD and those of ZL exhibit the same vertical extension to the red clump, yet we reach different conclusions as to the origin of the VRC despite using the same isochrones from Bertelli et al. (1994) with the same metallicity $Z = 0.008$ and helium abundance $Y = 0.25$. Why do our conclusions differ? ZL choose an isochrone with an age of $\log(\text{Age})=9.4$ as the best match to the red giant morphology of their un-dereddened CMD. They then note that although younger isochrones with $\log(\text{Age})=8.6$ can reproduce the increased luminosity of 0.9 mag observed in the VRC, the evolutionary models of Bertelli et al. predict a difference in color of the mean locus of the core He-burning phase of $\Delta(B - V) = 0.13$ mag, $\Delta(B - I) = 0.23$ mag between these two isochrones. Since they observe a color difference ≤ 0.07 in $B - I$ between the VRC and the centroid of the red clump, they dismiss stellar evolution as the origin of the VRC. They further note that the maximum change in luminosity predicted by Sweigart (1987) for stars evolving in the clump is 0.6 mag compared with the 0.9 mag that they observe in their CMD.

If the CMD are first dereddened before comparing to model isochrones, and the LMC is assumed not to be coeval but to have resulted from star formation that has been relatively constant over the last few Gyr, one reaches a different conclusion. Fig. 3 shows how the mean V magnitude of the core He-burning clump varies as a function of its $B - V$ color for stars of different ages using the models of Bertelli et al. (1994). Indeed, as noted by ZL, a measurable color difference is expected between stars of $\log(\text{Age})=8.6$ and $\log(\text{Age})=9.4$. However, as demonstrated by our Figs. 4 and 5, stars as old as 2.5 Gyr ($\log(\text{Age})=9.4$) do not fit the dereddened red clump at all, and for some of our fields appear to be too red to fit the bulk of red giant branch as well. Dereddening by even 0.12 mag (comparable to the average *foreground* reddening of our LMC fields) has a dramatic effect on the conclusions since this shifts the mean age of the clump to younger ages for which the luminosity of the blue loops is a very strong function of age, while the color does not change appreciably. Thus, allowing for a small range in the ages of young stars in the red clump is sufficient to reproduce the vertical extent of the VRC without significantly modifying its color. Note that this color insensitivity of the blue loops to age for stars between about 400 Myr and 1 Gyr is also true for the color defined by ZL ($C \equiv 0.565 * (B - I) + 0.825 * (U - V + 1.15)$), as shown in Fig. 9 for regions of the CMD comparable to that shown by ZL in their Fig. 1.

Zaritsky & Lin note that if the foreground population hypothesis is correct for the origin of the VRC, then the entire LMC CMD should show traces of a parallel CMD shifted by 0.9 mag. They can find no such traces in their own data, but do point to the HST color-magnitude diagram of Holtzman et al. (1997) as corroborating evidence that such a parallel feature may be present in the lower main sequence of the LMC. They rightly note

that binary stars would be a natural explanation for this excess of stars displaced by about -0.8 mag from the primary main sequence, but dismiss such an explanation as unappealing since it cannot simultaneously explain the VRC, where fine-tuning would be required to ensure that both members of the binary arrive in this region of the CMD at the same time. ZL conclude that if binaries are invoked as an explanation for the excess population in the lower main sequence, another explanation is necessary for the VRC. While we make no claims as to the origin of a parallel main sequence in the LMC, we do proffer stellar evolution as the required alternate explanation for the VRC.

5. Conclusions

Using BVR color magnitude diagrams obtained in four different regions in the LMC, we confirm the presence of a vertical extension of the red clump having the same color as the clump peak, but extending to brighter magnitudes, as first mentioned by Zaritsky & Lin (1997). Unlike ZL, however, we conclude that this feature is due to stellar evolution, not a foreground population. Our argument is based on noting that the feature (1) is present in all our LMC fields, (2) is in precise agreement with the time-averaged locus the blue loops that represent a relatively long-lived phase in the stellar evolution of younger core He-burning stars in the clump, (3) has a relative stellar density consistent with the density on the main sequence and the assumption of continuous and constant star formation history in the LMC over the past 1 Gyr, and (4) is present in the solar neighborhood as demonstrated by the Hipparcos color-magnitude diagram.

The difference in our conclusions despite using the same model isochrones (Bertelli et al. 1994) rests on differences in our reddening corrections and assumptions about the ages of LMC stars. ZL perform no reddening correction, whereas we correct for reddening using well-determined foreground estimates with a small correction for internal reddening based on main sequence fitting. This results in an average inferred $E(B - V) = 0.14$, only 0.02 mag greater than the average deduced for foreground extinction alone. ZL consider a single age of 2.5 Gyr for the clump with one possible burst at 400 Myr; we consider a population more distributed in age and weighted toward younger ages than ZL. An isochrone of 2.5 Gyr does not provide a good fit to the red clump in any of our fields, whereas the presence of younger stars in all our LMC fields is clearly demonstrated by comparison of isochrones with the position of the clump and the stellar density of the upper main sequence. We find that stars of ages $\sim 0.4 - 0.6$ Gyr are responsible for nearly the full extent of the VRC.

The best fit to both the main sequence and red clump of our CMD require a distance

modulus to the LMC of $\mu_{LMC} = 18.3$, assuming that the agreement of evolutionary models to the CMD of solar neighborhood can be taken to imply that no large systematic offset in luminosity is present in the theory.

With our justified assumption of continuous and constant star formation over the last Gyr in the LMC, current understanding of stellar evolution predicts with precision not only the position of the VRC seen in both our data and those of ZL, but also its relative stellar density. The same stellar evolutionary models (with appropriate assumptions for solar-metallicities) reproduce the VRC feature in the solar neighborhood CMD measured by the Hipparcos satellite. These models when applied to the LMC with a Salpeter IMF can account for $\sim 75\%$ of stellar density of the VRC compared to that of the upper main sequence. A slightly steeper IMF slope, such as preferred by many recent luminosity function studies of the LMC, reproduces the observed VRC stellar density exactly. Even with the Salpeter IMF, only one of our four fields (F1) contains VRC stars 1.5σ in excess of expectations from stellar evolution and simple assumptions for the star formation history of the LMC. Since microlensing events are currently being reported both in the bar and outer regions of the LMC, the 4σ discrepant bar field alone cannot contain a significant fraction of the microlensing optical depth to the LMC in the form of intervening stellar population. Indeed three of our four fields (F1, F2 and F3) contain a known microlensing candidate and thus have non-negligible optical depth to microlensing.

We conclude that no foreground population need be invoked to explain the presence of the vertical extension to the red clump in the LMC. If present, such a population is unlikely to account for more than $\sim 25\%$ of the VRC since the presence of intermediate mass LMC stars in the VRC are *required* by stellar evolutionary models in the observed numbers. Whatever the primary source of the measured microlensing optical depth toward the LMC, it is unlikely to be due to a new foreground population that has made its presence evident in this vertical extension of the red clump.

We thank Konrad Kuijken for useful discussion and a prompt yet careful reading of the manuscript. We are grateful to Andrew Cole for pointing out an error in an early version of this work and to Carme Gallart and Alvio Renzini for discussions about the AGB. We also thank Eric Maurice and Louis Prévot for advice on calibration procedures and Richard Naber for with DOPHOT subtleties. This work is based on observations carried out at the European Southern Observatory, La Silla. Work by PDS while at the Institute for Advanced Study in Princeton was supported by the NSF grant AST- 92-15485.

Note Added in Proof: The red clump is an increasingly popular distance indicator; two recent studies also find a smaller LMC distance (Udalski et al. 1998, Stanek et al. 1998).

REFERENCES

- Alcock et al. (The MACHO Collaboration) 1997a, *ApJ*, 486, 697
- Alcock et al. (The MACHO Collaboration) 1997b, *ApJ*, 490, L59
- Beaulieu J.P. et al. (The EROS Collaboration) 1995, *A&A*, 299, 168
- Bertelli, G., Bressan, A., Chiosi, C., Fagotto, F. & Nasi, E. 1994, *A&AS*, 106, 275
- Bennett, D. 1997, *ApJ*, 493, L79
- Cannon, R. D. 1970, *MNRAS*, 150, 111
- Chiosi, C., Bertelli, G. & Bressan, A. 1992, *ARA&A*, 30, 235
- de Vaucouleurs, G. 1957, *AJ*, 62, 69
- Elson, R.A.W., Gilmore, G.F. & Santiago, B.X. 1997, *MNRAS*, 289, 157
- Fusi Pecci, F., Ferraro, F.R., Crocker, D.A., Rood, R.T. & Buonanno, R. 1990, *A&A*, 238, 95
- Fagotto, F., Bressan, A., Bertelli, G. & Chiosi, C. 1994, *A&AS*, 105, 29
- Gallagher J. et al. 1996, *ApJ*, 466, 732
- Gallart, C. 1998, *ApJ*, 495, L43
- Gallart, C. & Bertelli, G. 1998, Proceedings of the Bonn/Bochum Graduiertenkolleg Workshop “The Magellanic Clouds and other Dwarf Galaxies,” Eds. T. Richtler & J.M. Braun, in press.
- Geha, M.C. et al. 1997, preprint, astro-ph/9711144
- Girardi, L., Chiosi, C., Bertelli, G. & Bressan, A. 1995, *A&A*, 298, 87
- Gould, A. 1997, preprint, astro-ph/9709263
- Graham J.A. 1982, *PASP*, 94, 244
- Holtzman, J. et al. 1997, *AJ*, 113, 656
- Jimenez, R., Flynn, C. & Kotoneva, E. 1997, submitted to *MNRAS*, also astro-ph/9709056
- Johnston, K.V. 1998, *ApJ*, 495, 297

- Minniti D. et al. 1997, in the Proceedings of the UC Santa Cruz Conference on *Galactic Halos*, ed. D. Zaritsky, to appear in PASP
- Olszewski, E.W., Suntzeff, N.B. & Mateo, M. 1996, ARA&A, 24, 511
- Paczynski, B. & Stanek, K.Z. 1998, ApJ, 494L, 219
- Perryman et al. 1995, A&A, 304, 69
- Perryman et al. 1997, A&A, 323, L49
- Renault C. et al. (The EROS Collaboration) 1997, A&A, 324, L69
- Renzini, A. & Fusi Pecci, F. 1988, ARA&A, 26, 199
- Rood, R.T. 1972 ApJ, 177, 681
- Salpeter, E.E. 1955, ApJ, 121, 161
- Schechter P., Mateo M. & Saha A, 1993, PASP, 105, 1342
- Schwering, P.B.W. & Israel, F. 1991, A&A, 246, 231
- Stanek, K.Z., Zaritsky, D. & Harris, J. 1998, submitted to ApJ, astro-ph/9803181.
- Sweigart, A.V., Greggio, L. & Renzini, A. 1989, ApJS, 69, 911
- Sweigart, A.V. 1987, ApJS, 65, 95
- Udalski A., Szymanski, M., Kubiak, M., Pietrzynski, G., Woziak, P. & Zebrun, K. 1998, Acta Astron., in press, astro-ph/9803035.
- Vallenari A., et al. 1996, A&A, 309, 367
- Vigneau J. & Azzopardi M. 1982, A&AS, 50, 119
- Zaritsky, D. & Lin, D.N.C. 1997, AJ, 114, 2545 (ZL)
- Zhao, H.-S. 1996 preprint, submitted to MNRAS, and astro-ph/9606166
- Zhao, H.-S. 1998, MNRAS, 294, 139

Figure Captions

Fig. 1 — Calibrated, composite $(V - R) - V$ color-magnitude diagrams for all four LMC fields described in the text. Only the 16,139 stars with cosmetically superior point spread functions (DOPHOT type 1) in V and R are plotted. Both uncorrected (left) and dereddened (right) CMD are shown. Positions of the red clump (RC), vertical extension to the red clump (VRC), and the supra-clump are indicated.

Fig. 2 — Calibrated, dereddened $(V - R) - V$ color-magnitude diagrams for the individual four LMC fields. Only stars with cosmetically superior point spread functions in V and R are plotted. The number of stars plotted is 3614, 4241, 5591, 2693 in $V - R$ for fields F1 through F4 respectively.

Fig. 3 — Centroid of the V -band luminosity of the core He-burning phase as a function of $B - V$ for stars of differing ages with LMC metallicity and helium abundance of $Z=0.008$ and $Y = 0.25$ (Bertelli et al. 1994). Note that no significant color change occurs for stars with ages between 400 Myr and 600 Myr; these stars correspond to the bulk VRC in the LMC. A similar sequence for $Z=0.02$ and $Y=0.28$ (appropriate to the solar neighborhood) yields a $B - V$ color redder by $\sim 0.1\text{mag}$ and is shown in Fig. 8. In the solar neighborhood, older stars are also present, causing the horizontal dispersion in color on the fainter edge of the red clump in the Hipparcos data.

Fig. 4 — **Top panel:** Calibrated, dereddened $(B - V) - V$ color-magnitude diagram for our least crowded field F2. 4666 stars with cosmetically superior point spread functions in B and V are shown. Isochrones with LMC metallicity ($Z = 0.008$) and helium abundance ($Y = 0.25$) with ages $\log_{10}(\text{Age}) = 8.4, 8.6, 8.8, 9.0,$ and 9.4 from Bertelli et al. (1994) are shown superposed for two different assumptions for the distance modulus, μ_{LMC} to the LMC. **Bottom panel:** Contour representation of the CMD density for field F2 in region of the red clump shown superposed on the mean locus of the core Helium burning phase as a function of age as in Fig. 3. Separate scales for the abscissa of the top and bottom panels are indicated. The region of CMD shown has been divided into 25 bins along both the magnitude and color axes. For this binning, contour levels displayed are 12, 10, 8, 6, 4 and 2.5 stars. A shorter distance modulus of $\mu_{LMC} = 18.3$ provides improved fits to the main sequence and red clump.

Fig. 5 — Calibrated, dereddened $(V - R) - V$ color-magnitude diagrams for each field as in Fig 2 with the isochrones from Fig. 4 overplotted. Here, and in what follows, $\mu_{LMC} = 18.3$ is assumed.

Fig. 6 — Same as the bottom panel of Fig 4, but for all of our LMC fields. The region of CMD shown has been divided into 25 bins along both the magnitude and color axes. For this binning, contour levels displayed are 25, 20, 15, 12, 10, 8, 6, 4 and 2.5 stars. The highest contour levels are not always present in the outer fields.

Fig. 7 — Histograms of main sequence stars for each of our fields are shown on a logarithmic scale. The number of stars in each magnitude bin expected from a Salpeter IMF, taking into account the main sequence lifetime and assumed a constant star formation rate over the last 1 Gyr, is shown as the solid sloping line. The normalization has been adjusted to achieve a good fit to the bulk of the main sequence stars between $16.5 < V < 18.5$. The faintest VRC and main sequence stars used for the counting arguments of §2.3.2 are indicated by the vertical lines at $V = 18.5$ and 19.5 , respectively. The main sequence counts clearly suffer from some incompleteness, whereas the VRC counts do not. Comparison with expectations from the Salpeter IMF produce the main sequence completeness estimates C_{MS} indicated for each field.

Fig. 8 — **Top panel:** Hipparcos $(B - V) - V$ color-magnitude diagram containing over 16000 stars with accurate distances and photometry. A vertical extension can be seen clearly on the blueward side of the red clump with nearly the same color as the peak clump density and extending about a magnitude brighter. The redder supra-clump is also visible. Isochrones with solar metallicity ($Z = 0.02$) and $\log_{10}(\text{Age})$ 8.6, 9.0, 9.4, 9.8 and 10.0 are shown overplotted. Note that positions of the blue loops again coincide with the vertical extension. **Bottom panel:** Contour representation of the CMD density in region of the red clump for the solar neighborhood as measured by Hipparcos is shown superposed on the mean locus of the core He-burning phase as a function of age for stars with metallicity and helium abundance appropriate to the solar neighborhood ($Z = 0.02$ and $Y = 0.28$). Separate scales for the abscissa of the top and bottom panels are indicated. The region of CMD shown has been divided into 20 bins along both the magnitude and color axes. For this binning, contour levels displayed are 35, 25, 15, 10, 5 and 2.5 stars.

Fig. 9 — The same isochrones of LMC metallicity from Fig. 3 are plotted in color-magnitude diagrams for the region of the red clump. The color $C \equiv 0.565*(B-I) + 0.825*(U-V + 1.15)$ is that used by Zaritsky & Lin (1997) as are the bands on the vertical axis: U (top), B (middle), and I (bottom) respectively. Reddening vectors assuming an average $E(B - V) = 0.12$ are shown in each panel. The blue loops correspond with the feature seen by ZL at a dereddened color of $C \approx 2.9$.

Table 1: Field center, seeing, and reddening determined from foreground and main-sequence fitting for each field.

Field	RA (J2000)	Dec (J2000)	Seeing	$E(B-V)_f$	$E(B-V)_{ms}$
F1	5h 26' 34"	−70° 57' 45"	1.0"	0.18	0.18
F2	5h 06' 05"	−65° 58' 03"	1.3"	0.08	0.12
F3	5h 14' 44"	−68° 48' 00"	1.0"	0.12	0.16
F4	5h 23' 00"	−66° 58' 00"	1.3"	0.12	0.12

Table 2: Position of the clump, relative limits of its vertical extension (VRC), and relative position of the supra-clump.

	F1	F2	F3	F4
Red Clump				
V_0	18.67 ± 0.03	18.65 ± 0.02	18.68 ± 0.03	18.70 ± 0.02
$(B - V)_0$	0.87 ± 0.01	0.86 ± 0.01	0.85 ± 0.01	0.88 ± 0.02
$(V - R)_0$	0.48 ± 0.01	0.48 ± 0.01	0.48 ± 0.01	0.48 ± 0.01
VRC				
δV_0	-0.80 ± 0.05	-0.82 ± 0.05	-1.02 ± 0.05	-0.63 ± 0.10
$\delta(B - V)_0$	-0.01 ± 0.01	0.01 ± 0.01	0.01 ± 0.01	0.00 ± 0.02
$\delta(V - R)_0$	0.00 ± 0.01	-0.02 ± 0.01	0.00 ± 0.01	0.00 ± 0.02
Supra Clump				
δV_0	-0.82 ± 0.05	-0.85 ± 0.05	-0.84 ± 0.05	-0.86 ± 0.05
$\delta(B - V)_0$	0.24 ± 0.02	0.24 ± 0.02	0.20 ± 0.02	0.25 ± 0.02
$\delta(V - R)_0$	0.10 ± 0.02	0.11 ± 0.02	0.10 ± 0.02	0.10 ± 0.01

Table 3: Number counts and relative fractions of the vertical extension to the red clump (VRC), supra-clump (SC), and red clump (RC) in the individual and composite fields. See §2.1.2 for the operative definition used here for each of these regions in the CMD.

Field	VRC	SC	RC	VRC/RC	SC/RC
F1	45	92	777	6%	12%
F2	39	34	261	15%	13%
F3	97	176	1074	9%	16%
F4	19	49	330	6%	15%
Comp	200	351	2442	8%	14%

This figure "beaulieusackett.fig1.gif" is available in "gif" format from:

<http://arxiv.org/ps/astro-ph/9710156v2>

This figure "beaulieusackett.fig2.gif" is available in "gif" format from:

<http://arxiv.org/ps/astro-ph/9710156v2>

This figure "beaulieusackett.fig3.gif" is available in "gif" format from:

<http://arxiv.org/ps/astro-ph/9710156v2>

This figure "beaulieusackett.fig4.gif" is available in "gif" format from:

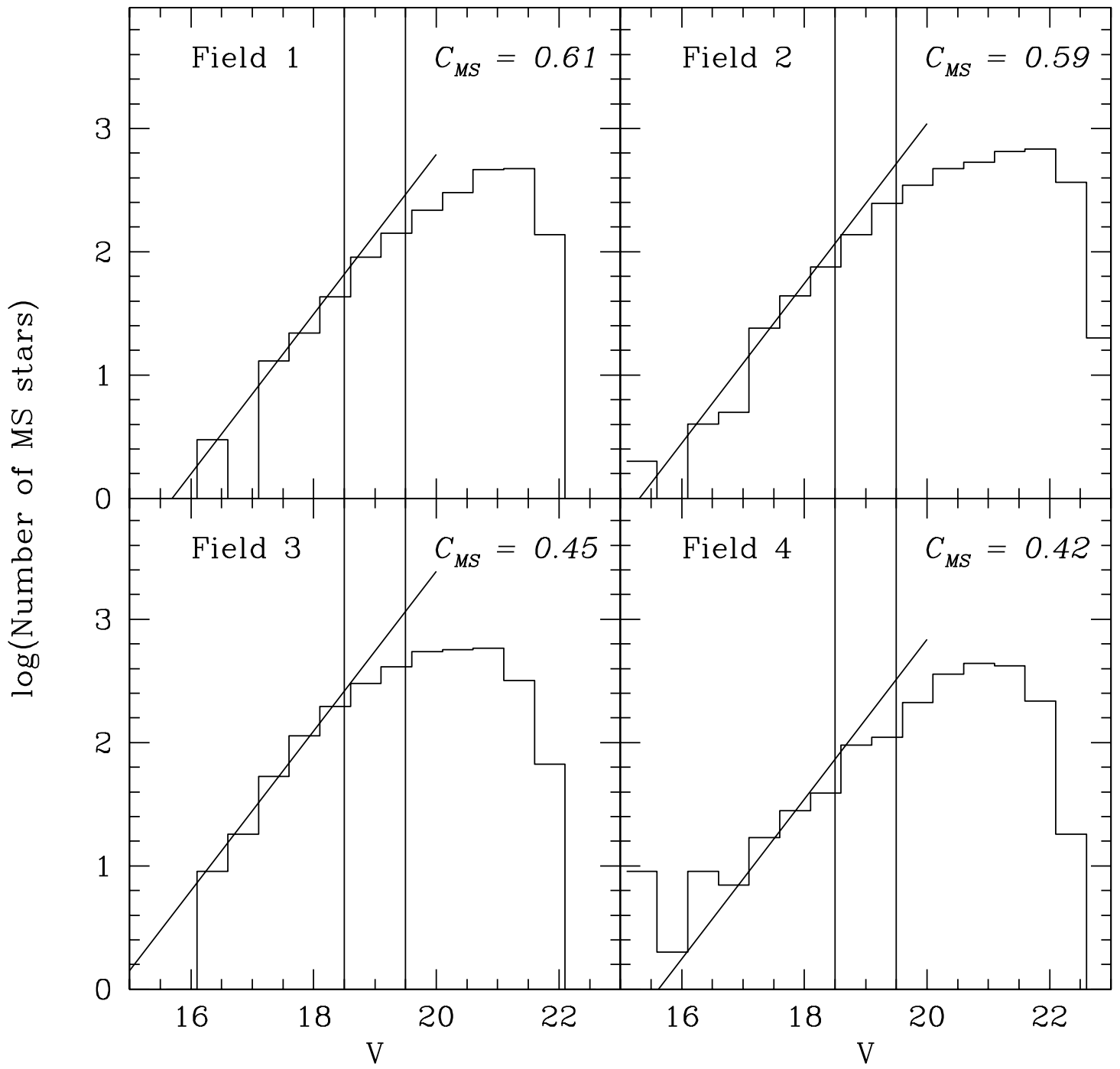
<http://arxiv.org/ps/astro-ph/9710156v2>

This figure "beaulieusackett.fig5.gif" is available in "gif" format from:

<http://arxiv.org/ps/astro-ph/9710156v2>

This figure "beaulieusackett.fig6.gif" is available in "gif" format from:

<http://arxiv.org/ps/astro-ph/9710156v2>



This figure "beaulieusackett.fig8.gif" is available in "gif" format from:

<http://arxiv.org/ps/astro-ph/9710156v2>

This figure "beaulieusackett.fig9.gif" is available in "gif" format from:

<http://arxiv.org/ps/astro-ph/9710156v2>